

# Dynamic Aeroelastic Response of Buffeting in V-Tail Empennage

kalaiyarasan.N<sup>1</sup> and Sankar.V<sup>2</sup>

<sup>1</sup> PG Scholar, kalaiyaeronaughty@gmail.com

<sup>2</sup> Professor, sankar101@gmail.com

Department of Aeronautical Engineering, Nehru Institute of Engineering and Technology  
Coimbatore, Tamil Nadu

## Abstract

The main objective of this article is to predict the buffeting in the tail which helps in preventing the structural failure. The proposed V-tail model is drafted using modelling software and flow analysis and structural analysis is carried out using CFD and FEA tools. The V-tail model has been analyzed at certain constant altitude in compressible subsonic range using optimization CFD and FEA tools. The deformation exist in a V-tail model caused by dynamic aero elastic effects. The resulted pressure value is used as input to the structural analysis and the corresponding structural deformation is studied and validated.

**Keywords:** aeroelasticity, deformation, buffet, v-tail, stress variation.

## 1. Introduction

In general aircraft will suffer aeroelastic problems during flight operations. Aero elastic instabilities are caused by the unfavourable interaction between inertial, elastic and aerodynamic forces dwelling on aircraft structures. The interplay generates unstable oscillation that may sometimes lead to structural failures<sup>[1]</sup>. Aeroelastic analysis is based on the coupling of a structural dynamics model and on aerodynamic model, the structure is modeled by a finite element model, and the aerodynamics is modeled by a linear panel aerodynamic model<sup>[2]</sup>.

In this article, the aeroelastic response predicted in terms of deformation and stress distribution over a V-tail model. There are two ways to calculate fluid structural interaction i.e., strongly coupled fluid structural interaction and partly coupled fluid structural interaction<sup>[3]</sup>.

### 1.1 Aeroelastic effects Prediction

The aeroelastic effect occurring on a V-Tail due to the flow separation is considered for the present analysis. The prediction of aerodynamic forces and their influence is done using a three-dimensional N-S model with fully coupled iterations to identify the confusing physical phenomena. Once the flow field solutions are converged, then the flexural motion of the tail caused by the influence of aerodynamic forces will be computed. The Algorithm for the proposed analysis is presented in Fig (1)<sup>[4]</sup>.

The aerodynamic forces are solved by using flow field governing equations and the structural displacement are solved by using structural governing equations as shown in figure1.

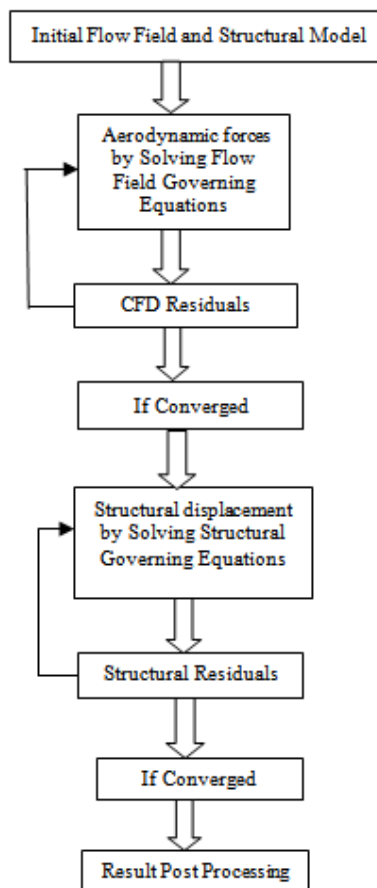


Figure. 1 Algorithm for partially coupled for fluid structural interaction analysis<sup>[4]</sup>

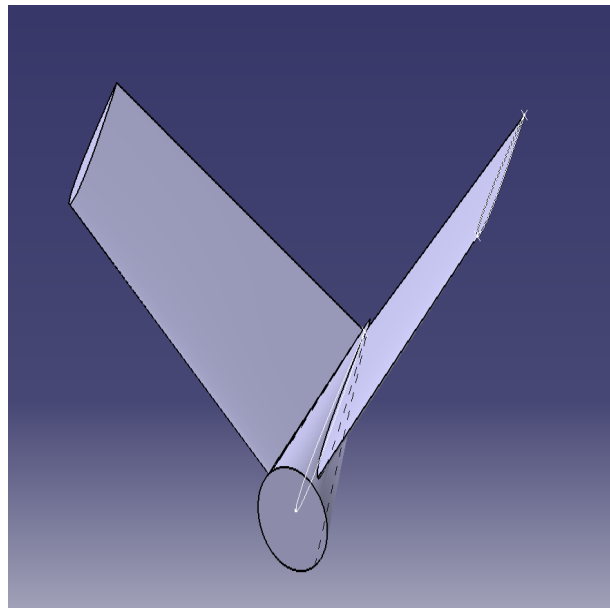
## 2. Model Description

The proposed V-tail model is built by using NACA four series, NACA 0006 with 6% of maximum thickness at 30% of chord and 0% of camber. The V-tail model is drafted using modelling software. The specification for the proposed V-tail model is tabulated in table I.

*Table 1: Specification of V-tail*

Sl. NO.	PARAMETERS OF MODEL	TYPES AND DIMENSIONS
1.	Tail type	V-tail
2.	Airfoil type	NACA 0006 airfoil
3.	Root chord	1.43m
4.	Tip chord	0.972m
5.	Tail span length	3.212 m
6.	Taper ratio	5°
7.	Dihedral angle	39.5°

Using the specification which is tabulated in table I, the V-tail model is designed using modelling software. The designed V-tail model is shown in figure 2.

*Figure. 2 Drafted model of a V-tail in 3D view*

## 2.1 Grid Generation

A C-Domain control volume is used for better flow field analysis. A fine tetrahedron mesh is generated for both the control volume and V-tail model as shown in figure 3. Tetrahedron grid is preferred for 3-D solid structures for flow analysis. Totally 57962 nodes and 322608 elements are generated for the control volume which is used for flow field analysis as shown in figure 3.

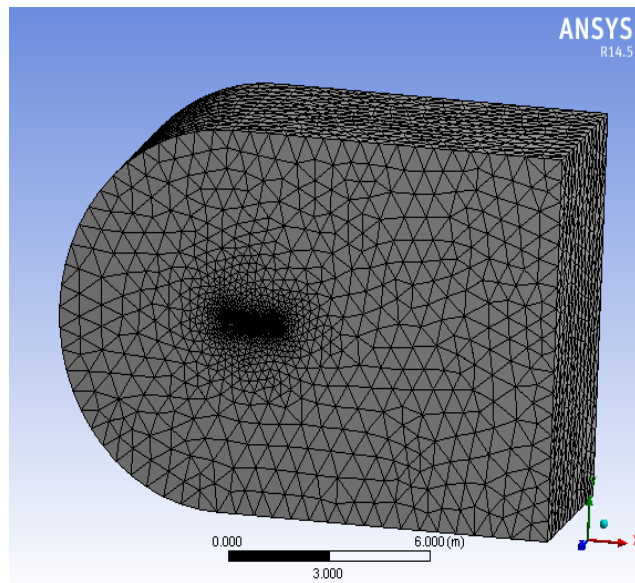


Figure 3: Meshed model of a Control Volume

## 2.2 Boundary Conditions

The numerical values of the boundary conditions are given as the International Standard Atmospheric (ISA) properties at 6 km altitude which is shown in Table II<sup>[12]</sup>. The velocity range is considered from 0.35 Mach to 0.6 Mach. The control volume is considered to be fluid body where the flow is to be analysed. The tail model is considered as solid body over which the flow occurs. Numerical analysis is carried out using analysing software. Numerical analysis is carried out with the information tabulated below.

Table2:International standard atmospheric (ISA) properties at 6 km altitude

SI.NO	VARIABLES	ISA PROPERTIES
1.	Temperature	249.2 K
2.	Pressure	47217 pa
3.	Density	0.6601 kg/m <sup>3</sup>
4.	Viscosity	1.601E-5 kg/ms
5.	Speed of sound	316.4309 m/s

Since there is an option of symmetry in analyzing software the drafted V-tail can be sliced to symmetry for saving time. One half of the V-tail is fixed to the axis and considered for numerical analysis. The imported pressure load from the fluid flow solver is applied on the fluid- solid interface face.

### 3. Results and Discussions

The main objective of modal analysis is to determine the dynamic characteristics of V-tail such as natural frequency and mode shapes. The vibrational analysis of the v-tail is carried out using analyzing software.

*Table 3: Natural frequency of a v-tail*

MODE	FREQUENCY (Hz)
1	17.579
2	67.066
3	79.923
4	144.67
5	181.19
6	246.71
7	247.51
8	285.45
9	289.93
10	335.02

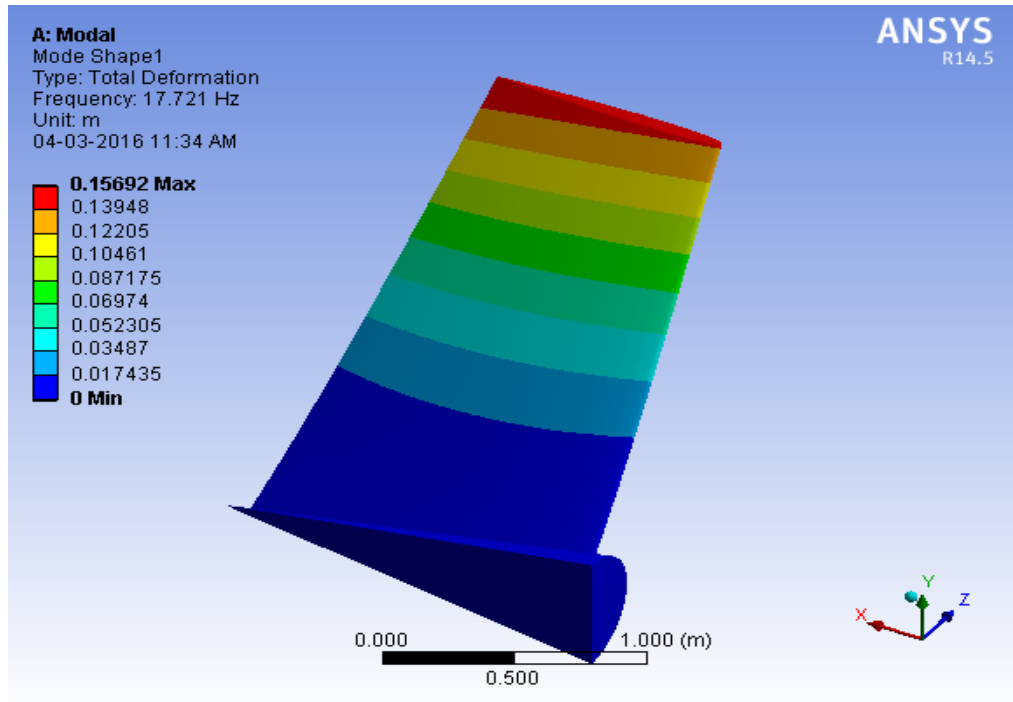


Figure4: Vector contour of Mode Shape 1

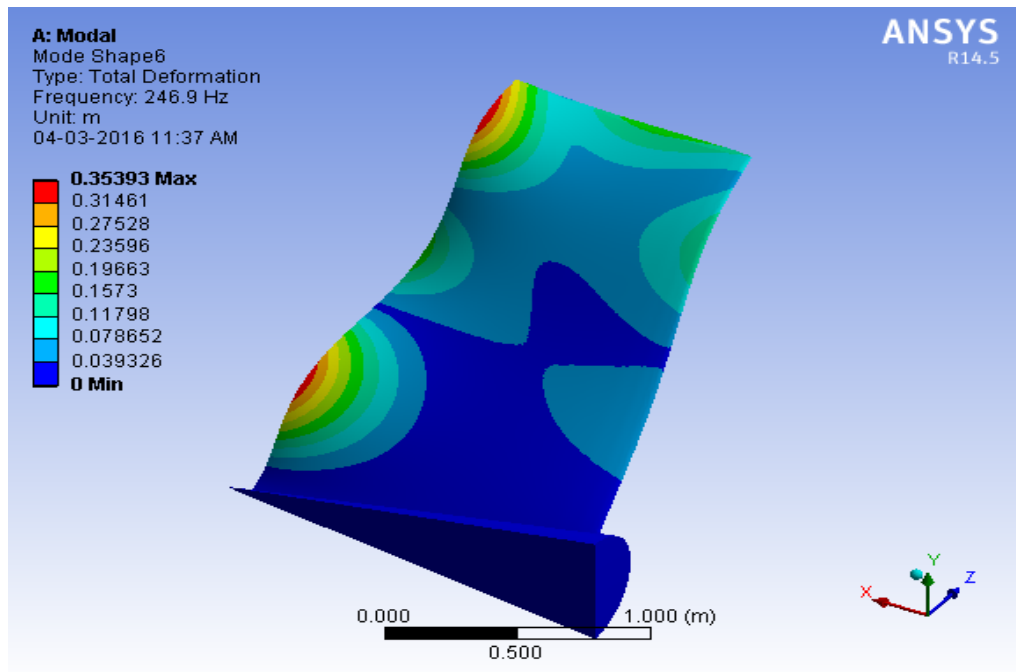


Figure 5: Vector contour of Mode Shape 6

The natural frequency value obtained from the vibrational analysis is tabulated in the table III. The mode shapes obtained during the modal analysis of V-tail for mode shape 1 and 6 is shown in figure 4 and 5. The flow field analysis are carried out for V-tail model at various Mach numbers from 0.35 to 0.6 using Computational fluid dynamics tool. In the flow field analysis, Static pressure distribution and turbulent kinetic energy variation around the V-tail model are computed by given boundary conditions for the post processing.

The maximum static pressure variation against Mach number is shown in figure 6. The static pressure variation over the tail at 0.4 Mach number is shown as contour in figure 7. The maximum and minimum static pressures obtained for the remaining velocity conditions similar to 0.4 Mach number are presented in Table IV

Table 4 :Maximum And Minimum Static Pressure Vs Mach Numbers

S.L.N O.	MACH NO.	MIN. PRESSURE (pa)	MAX. PRESSURE (pa)
1.	0.35	0.299071	4125.8
2.	0.4	0.371552	5436.8
3.	0.45	0.353318	6951.67
4.	0.5	0.4796	8680.9
5.	0.55	4.8271	10638
6.	0.6	3.62314	12840.1

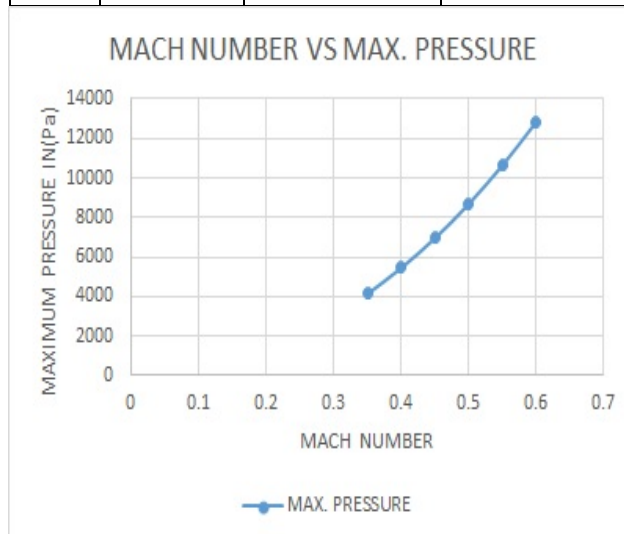


Figure 6: Maximum pressure variation about Mach number

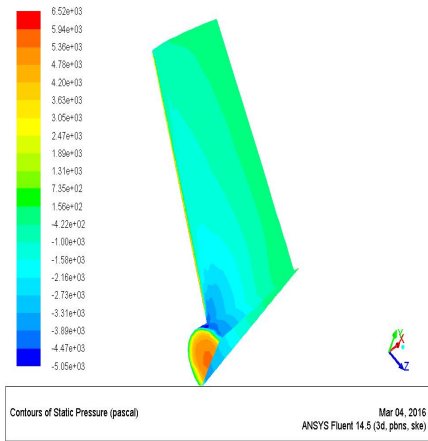


Figure7: Contour Static pressure variation at 0.4 Mach number

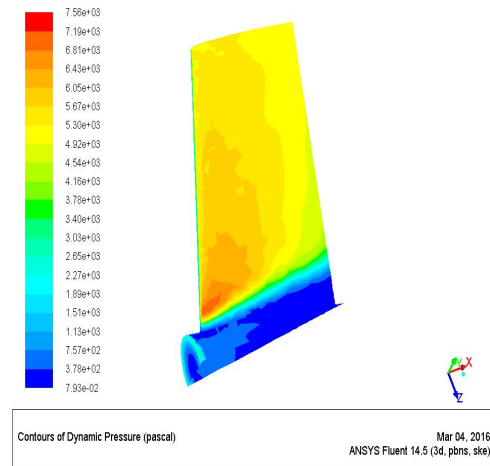


Figure 8: Contour dynamic pressure variation at 0.4 Mach number

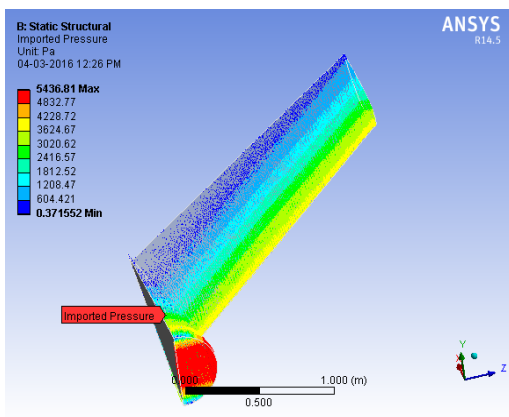


Figure9: Imported pressure load variation at 0.4 Mach number

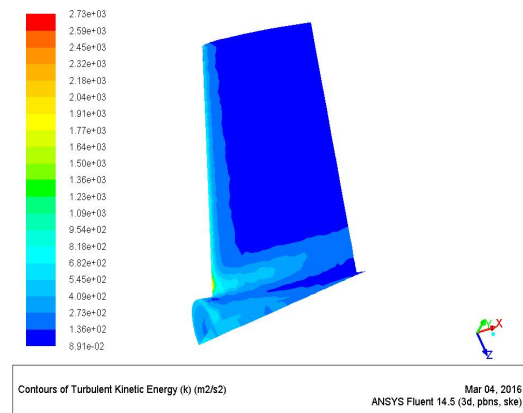


Figure 10: Turbulent kinetic energy variation at 0.4 Mach number



The following figure 11 and 12 provides the information about the imported pressure load distribution over the V-tail at Mach number 0.4. Also the following table V and figure 11 and 12 provides the information about the computed equivalent von – mises stress distribution over the V-tail at Mach number 0.35 to 0.6.

*Table 5 :Maximum And Minimum Von – Mises Stress Vs Mach Numbers*

SI. NO.	MACH NUMBER	MAX. STRESS (pa)	MIN. STRESS (pa)
1.	0.35	8146800	49.531
2.	0.4	11037000	60.26
3.	0.45	14510000	67.921
4.	0.5	18544000	36.851
5.	0.55	23133000	46.682
6.	0.6	28158000	24.425

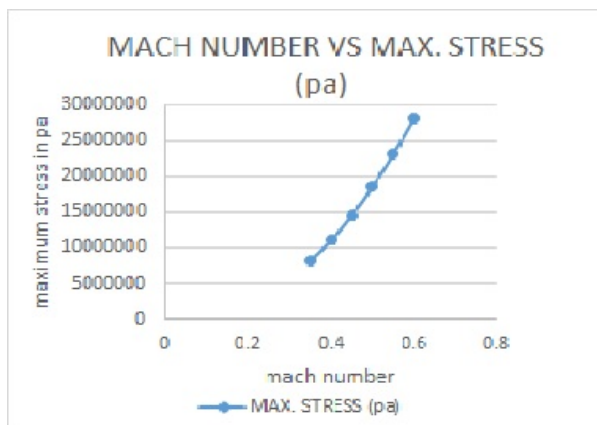


*Figure11: Maximum Stress variation about Mach number*

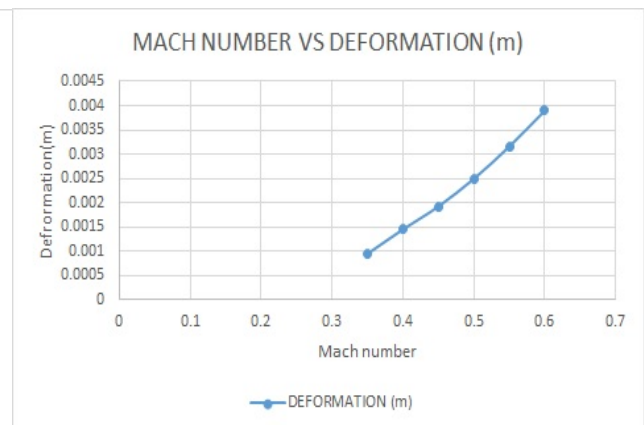


*Figure 12: Maximum Deformation variation about Mach number*

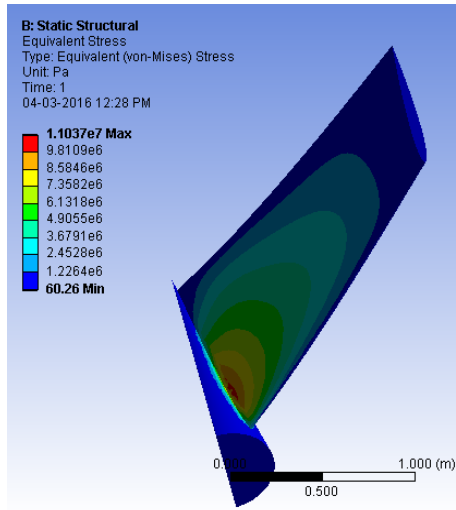


Figure 13: Computed Von - Mises Stress variations at 0.4 Mach number

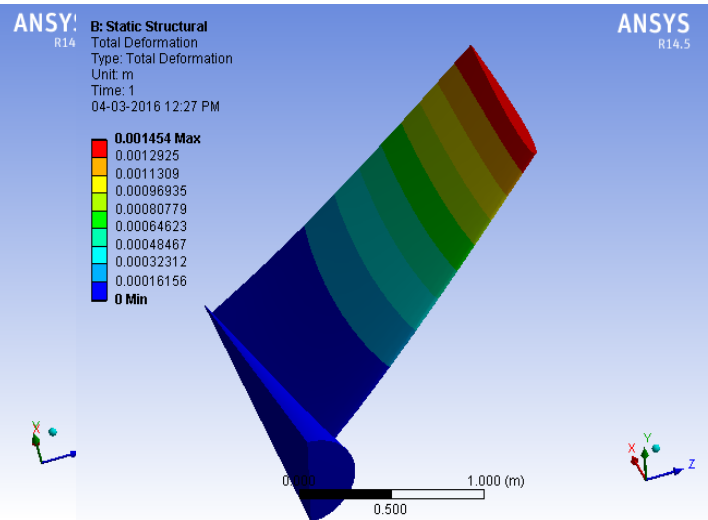


Figure 14: Total deformation contour at 0.4 Mach number

The total deformation produced on the V-tail because of the pressure load acting on it (0.4 Mach number) is shown in figure 14. The V-tail for various velocity inlet conditions deformations values are computed as illustrated and tabulated in figure 13 and table VI.

Table 6: Total Deformation Vs Mach Numbers

SI. NO.	MACH NUMBER	DEFORMATION (m)
1.	0.35	0.00095163
2.	0.4	0.001454
3.	0.45	0.0019263
4.	0.5	0.0024962
5.	0.55	0.0031616
6.	0.6	0.0038978

#### 4. Conclusion

The considered V-tail model is kept at  $0^\circ$  Angle of Attack throughout the analysis. Therefore, the pressure distributions obtained for the subsonic Mach numbers from 0.35 to 0.6 are verified with the available historical data. The results are fully agreed with the data exist in the NACA report and verified with the six inlet velocity conditions. From the results and contours, it is identified that the non-linear aeroelastic effects in subsonic velocities are negligible. The methodology used in this article can be implemented for conventional tail and T-tail with subsonic Mach numbers to study the aeroelastic nature of such designs.

#### References

- [1] A.Attorni,L.Cavagna,G.Quaranta (2011),”Aircraft T-tail flutter predictions using computational fluid dynamics” Elsevier. Journal of fluid and Structures 27 (2011) 161–174.
- [2] Daniella E. Raveh (2005), ‘Computational-fluid-dynamics-based aeroelastic analysis and structural design optimization—a researcher’s perspective’, Elsevier. Computer Methods in Applied Mechanic and Engineering. 194 (2005) 3453–3471.
- [3] C.Bibin, Micheal Johnson Selvaraj and S.Sanju (2012), ‘Flutter analysing over an aircraft wing during cruise speed’, Elsevier. Procedia Engineering 38 (2012) 1950 – 1961.
- [4] Manivel. M, Jinu. G. R, Bruce Ralphin Rose. J, (2014), “Partly Coupled Fluid Structure Interaction Analysis of an Aircraft Wing at Subsonic Speeds”, International Journal of Mechanical & Mechatronics Engineering IJMME-IJENS Vol: 14 No:03,pg .22-29.
- [5] V.D.Chuban,(2005),”Influence of angle of attack and stabilizer deflection on T-Empennage flutter”,Journal of aircraft vol.42,No.1,264-268.
- [6] Y.H.Zhao, H.Y.Hu (2009),”Active control of vertical tail buffeting by piezoelectric actuators”, Journal of aircraft, Vol.46.No.4.1167-1175.
- [7] Zhao Yong hui, HU Hai yan (2005), ‘Structural Modeling and Aeroelastic Analysis of High Aspect Ratio Composite Wings’, CHINESE JOURNAL OF AERONAUTICS, Vol. 18 No. 1, February 2005.
- [8] Nikhil A. Khadse and Prof. S. R. Zaveri (2015), ‘Modal Analysis of Aircraft Wing using Ansys Workbench Software Package’, International Journal of Engineering Research & Technology (IJERT) ISSN: 2278-0181 Vol. 4 Issue 07, July-2015.
- [9] Daniella E. Raveh (2005), ‘Computational-fluid-dynamics-based aeroelastic analysis and structural design optimization—a researcher’s perspective’, Elsevier. Computer Methods in Applied Mechanic and Engineering. 194 (2005) 3453–3471
- [10] Seong Hwan Moon, Seung Jo Kim (2003), ‘Suppression of nonlinear composite panel flutter with active/passive hybrid piezoelectric networks using finite element method’, Elsevier. Composite Structures 59 (2003) 525–533.
- [11] Justin W. Jaworski and Earl H. Dowell (2009), ‘Comparison of Theoretical Structural Models with Experiment for a High-Aspect-Ratio Aeroelastic Wing’, JOURNAL OF AIRCRAFT Vol. 46, No. 2, March–April 2009.
- [12] John D Anderson Jr, ‘Fundamentals of Aeronautics’, fourth edition McGraw Hill companies.
- [13] Y.C.Fung, ‘An introduction to aeroelasticity’, Dower publications, Inc, Newyork.
- [14] T.H.G.Megson, ‘Aircraft structures for engineering students’, Edward Arnold Publisher limited, ISBN : 0713133937

**A Brief Author Biography**

**Kalaiyaran.N** – Pursuing PG-Aeronautical Engineering in Nehru institute of Engineering and Technology, Coimbatore, Anna University, Chennai. Completed UG- Aeronautical Engineering in 2014 in SREC College of Engineering and Technology, Coimbatore, Anna University, Chennai.

**Sankar.V** – Working as professor in Department of Aeronautical in Nehru institute of Engineering and Technology, Coimbatore. He has got masters in aeronautical engineering and he is also pursuing PhD in material science.